Accepted Manuscript

Aromatic aldehyde based chemosensors for fluoride and cyanide detection in organic and aqueous medium: Ascertained by characterization, Spectroscopic and DFT Studies

Suresh N. Kodlady, B. Narayana, B.K. Sarojini, B.U. Gauthama

PII: S0020-1693(19)30259-2
DOI: https://doi.org/10.1016/j.ica.2019.05.030
Reference: ICA 18931

To appear in: *Inorganica Chimica Acta*

Received Date: 25 February 2019
Revised Date: 15 May 2019
Accepted Date: 16 May 2019

Please cite this article as: S.N. Kodlady, B. Narayana, B.K. Sarojini, B.U. Gauthama, Aromatic aldehyde based chemosensors for fluoride and cyanide detection in organic and aqueous medium: Ascertained by characterization, Spectroscopic and DFT Studies, *Inorganica Chimica Acta* (2019), doi: https://doi.org/10.1016/j.ica.2019.05.030

This is a PDF file of an unedited manuscript that has been accepted for publication. As a service to our customers we are providing this early version of the manuscript. The manuscript will undergo copyediting, typesetting, and review of the resulting proof before it is published in its final form. Please note that during the production process errors may be discovered which could affect the content, and all legal disclaimers that apply to the journal pertain.

ACCEPTED MANUSCRIPT

Aromatic aldehyde based chemosensors for fluoride and cyanide detection in organic and aqueous medium: Ascertained by characterization, Spectroscopic and DFT Studies.

Suresh N Kodlady, B. Narayana*, B. K. Sarojini**, B. U. Gauthama.

*Department of Studies in Chemistry, Mangalore University, Mangalagangothri -574199, Karanatka, India.

**Department of Industrial Chemistry, Mangalore University, Mangalagangothri -574199, Karanatka, India.

Graphical abstract

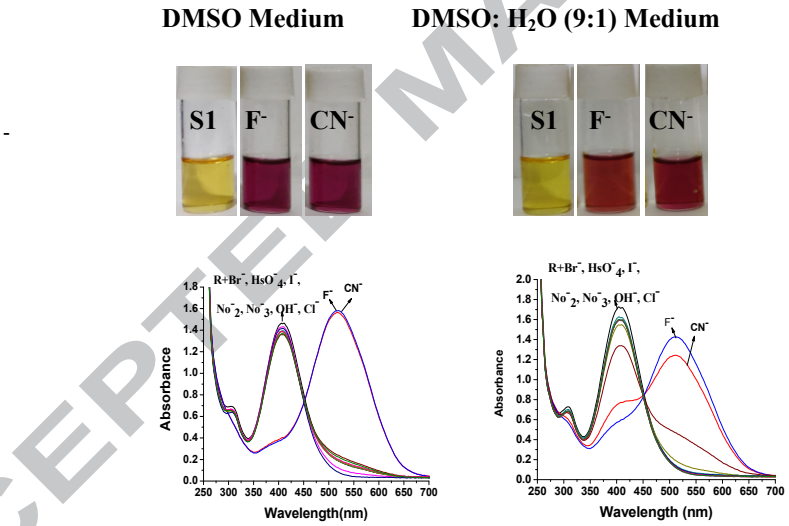

ABSTRACT

In the present investigation, a series of new aromatic aldehyde based chemosensors (S1-S4) have been sensibly designed and synthesized by the simple condensation reaction and their anion sensing properties were investigated. The compounds were characterized by spectroscopic techniques such as FT-IR, UV-Visible, ^{1}H NMR, ^{13}C NMR and ESI-MS. The probes exhibited high sensitivity and selectivity towards fluoride and cyanide ions over the anions such as Br^-, HSO^-_4, Cl^-, OH^-, I^-, NO^-_2 and NO^-_3 in dry DMSO and DMSO-water mixture (DMSO: H_2O 9:1

ACCEPTED MANUSCRIPT

v/v). The binding mechanism of fluorometric chemosensors with N-H-F and N-H-CN ion was determined based on ^{1}H NMR titration and were also theoretically supported by DFT (Density functional theory) calculation. The stoichiometry and binding constant (Ka) of the host-guest complexes formed were determined by the Benesi–Hildebrand (B–H) plot and Job's method respectively. Finally, economically visible paper-based colorimetric "test stripes" of (S1-S4) were fabricated to the detection of F^- and CN^- ions in 100% aqueous solution.

Keywords: Optical sensing, Fluoride ion, Cyanide ion, Colorimetric sensors, Organic medium, organo-aqueous medium.

1. Introduction

Fluoride and Cyanide have distinctive chemical and biological properties, particularly owing to its strong electro-negativity and small size. Considerable work has been designed for the synthesis of selective receptors for sensing of anions. Lower concentrations of fluoride ion have been devoted beneficial to avoid dental caries. At lower concentrations, the researchers are discussing the health benefits of fluoride ions[1-3]. Among the most interested biologically important anions, fluoride is of great importance because of its conventional role in the treatment of osteoporosis and dental care[4]. In many cases, sensing of cyanide ion is indispensable in environmental, biological and industrial research[5-6], such as gold extraction, plastic manufacturing, metallurgy and electroplating but at the same time it is highly noxious to human health even at very small concentration due to its strong interactions with the active site of cytochrome-oxidase[7-8]. For example, the fluoride ion is a major ingredient in hypnotics, anesthetics, rat and cockroach poisons, psychiatric drugs and military nerve gases[9-11]. The cyanide ion also detrimentally affects vascular, visual, central nervous, cardiac, endocrine and metabolic functions. However, cyanide toxicity, large quantities of cyanide salts are still widely used in industrial production such as metallurgy (1.5 million tons per year), electroplating and the synthesis of fine chemicals. With the importance of the industries, cosmetic goods of fluoride products, particularly food and food products, the contamination of fluoride is more dangerous[12]. Therefore sensing of fluoride and cyanide ions in the micromolar concentration in chemical, biological and environmental samples is outermost

ACCEPTED MANUSCRIPT

important[13-14]. Although several methods including atomic absorption, voltametric, potentiometric, electrochemical and ion exchange techniques have been explored these methods do not offer a cost-effective, rapid and real-time monitoring system for fluoride and cyanide ions.

Fluoride is the smallest and the outmost important electronegative atom and has peculiar chemical properties and can form the strongest hydrogen-bond donor[15-16]. In particular, the synthesis of colorimetric anion sensors is most important why because visual detection can propose qualitative and quantitative information at low levels and broadly used due to its low cost or no requirements of specific equipment [17-18]. Chemosensors are developed according to the chromophore receptor general binomial[19-20], which associate with the binding of a specific anion substrate with receptor sites and a chromophore responsible for transforming the receptor anion complex particularly participation into an optical signal when anions communicate with the anion sensors through hydrogen bonding, electrostatic, hydrophobic interaction, coordination to a metal center, or a combination of any two or more of these interactions. The anion sensor can yield binding information either by its altered fluorescence, absorption spectra or both behaviors [21-25]. The color variation can be associated with either structural or conformational changes in the receptor moiety when a complex is formed or to the formation of charge transfer complex[26]. These schemes are based upon N-H proton transfer from the donor entity to an anion, which induce N-H deportation or π-electron delocalization[27]. Considerable efforts have been made to develop hydrogen bonding receptors containing amine[28], imidazole ion[29], urea[30-31], thiourea[32-33], imine[34], phenol[35-36], pyrole[37-37], hydroxyl groups[39] and hydrazones[40]. In the present study, design and synthesis of chemosensors based on reaction of aldehyde with amine, forming a Schiff base (-C=N-) as a bridge was attempted [41].

In the synthesis of selective fluoride and cyanide ion chemosensors, aromatic aldehyde receptor (S1-S4) was synthesized by the condensation of an aldehyde and 2,4 dinitrophenyl hydrazine, this is an organic colorimetric chemosensor. The sensing of the fluoride and cyanide ion was developed in DMSO and DMSO: H_2O (9:1). This result shows the fluoride and cyanide ions can be detected by the naked eye without interference from other anions based on N-H proton transfer. The details of anion binding specific aromatic aldehyde with 2,4 dinitrophenylhydrazine (S1-S4) have been analyzed by UV-Visible and DFT studies. These receptors (S1-S4) have high selectivity towards fluoride and cyanide ions in both spectroscopic and absorption modes.

ACCEPTED MANUSCRIPT

2. Experimental

2.1 Materials and methods.

All solvents and reagents (analytical grade and spectroscopic grade), all the anions in tetrabutylammonium salts were obtained from Merck (India) and spectrochem Pvt. Limited (India) and used without any further purification. All lab experiments were carried out at room temperature. All UV-Visible spectra were carried out in DMSO and DMSO: H_2O (9:1), NMR spectra of the pure samples were recorded using a Bruker Advance (400 MHz) spectrophotometer, where tetramethylsilane (TMS) was used as the internal standard and DMSO-*d6* and $CDCl_3$ as the solvent. Resonance multiplicities were explained as s (singlet), d (doublet), t (triplet), and m (multiplet). IR spectra were recorded on Bruker FT-IR spectrometer. Mass spectra were analyzed on a Waters Micromass Q-Tofmicro spectrometer with ESI source. UV-Vis spectra were recorded with a spectroquant pharo300 Spectrometer in standard 3.5 ml quartz cells with 1 cm path length. The progress of the reaction was monitored by TLC plates. Melting point was recorded on Raga melting-point apparatus in open capillaries[42].

1-(2,4-dinitrophenyl)-2-((E)-3-phenylallylidene) hydrazine S1

Melting point=248-250 ^oC. δ_H (400 MHz; DMSO-*d6*): 7.0-7.11 (s, 2H, ArH), 7.34-7.50 (m, 3H, ArH), 7.63-7.68 (t, 2H, ArH), 7.91-7.93 (d, 1H, *J*-9.2 Hz, ArH), 8.38– 8.40 (d, 1H, *J*-9.2 Hz, ArH), 8.47–8.49 (d, 1H, J-6 Hz, ArH), 8.85 (s, 1H, ArH), 11.5(s, 1H, NH, ArH) (Fig-A4). ^{13}C NMR (DMSO-*d6*): δ (ppm): 116.12, 116.47, 122.86, 123.00, 124.81, 127.26, 127.75, 128.89, 129.07, 129.20, 129.37, 129.79, 136.98, 140.48, 151.76 (Fig-A5). LCMS (ESI-MS) m/z: $[M-H]^-$ Calculated for $C_{15}H_{12}N_4O_4$, 312.09, Found: 310.95 (Fig-A3). FT-IR (KBr) ν (cm^{-1}) =3305, 3276, 3096, 3033, 1945, 1585, 1505, 1491, 1421, 1302, 1275, 1253, 1217, 1125, 1106, 1063, 1027, 972, 916, 873, 824, 737, 681, 63 (Fig-A2). Yield=85%.

3-((2-(2,4-dinitrophenyl) hydrazono)methyl) pyridine S2

Melting point= 258-260^o C. δ_H (400 MHz; DMSO-*d6*): 7.54 (dd, *J1*=4.4 Hz, J2=7.62 Hz, 1H, ArH), 8.10-8.26 (m, 2H, ArH), 8.30-8.49 (m, 1H, ArH), 8.66 (d, *J*=3.2 Hz, 1H, ArH), 8.77 (S,

ACCEPTED MANUSCRIPT

1H, ArH), 8.88 (S, 1H, ArH), 8.89 (S, 1H, ArH), 8.95 (S, 1H, ArH), 11.77 (S, 1H, ArH) (Fig-A17). ^{13}C NMR (DMSO-*d6*): δ (ppm): 116.96, 122.89, 124.08, 129.14, 129.85, 133.82, 137.42, 144.31, 146.49, 148.83, 150.99 (Fig-A18). LCMS (ESI-MS) m/z: [M-H]$^-$ Calculated for $C_{12}H_9N_5O_4$, 287.07, Found: 285.95 (Fig-A16). FT-IR (KBr) ν (cm^{-1}) =3296, 3093, 1616, 1581, 1510, 1419, 1323, 1267, 1220, 1143, 1082, 966, 925, 894, 831, 806, 740, 721, 702, 655, 582, 555, 532 (Fig-A15). Yield=91%.

4-bromo-2-((2-(2,4-dinitrophenyl) hydrazono)methyl) phenol S3

Melting point= 265-267^{o}C. δ_H (400 MHz; DMSO-*d6*: 6.89-6.91 (d, 1H, J=8.0 Hz, ArH), 7.45 (dd, J1=2.4 Hz, J2=8.4 Hz, 1H, ArH), 7.98-8.0 (d, J=8.0 1H, ArH), 8.11-8.813 (d, J=8.0,1H, ArH), 8.38-8.39 (d, J=4.0, 1H, ArH), 8.86-8.92 (m, 2H, 2H, ArH), 10.54 (S, 1H ,ArH), 11.77 (S, 1H, ArH) (Fig-A35). ^{13}C NMR (DMSO-*d6*): δ(ppm): 110.93, 116.95, 118.54, 122.46, 122.88, 127.85, 129.48, 127.72, 134.00, 137.03, 144.29, 144.34, 156.03 (Fig-A36). LCMS (ESI-MS) m/z: [M-H]$^-$ Calculated for $C_{13}H_9BrN_4O_5$, 379.98, Found: 380.90 (Fig-A34). FT-IR (KBr) ν (cm^{-1}) = 3292, 3093, 1614, 1581, 1510, 1475, 1415, 1388, 1328, 1305, 1274, 1261, 1219, 1184, 1147, 1107, 1058, 943, 918, 881, 831, 817, 740, 723, 655, 624, 557, 528 (Fig-A33). Yield=85%.

2-((2-(2,4-dinitrophenyl) hydrazono)methyl) phenol S4

Melting point= 252-254^{o}C. δ_H (400 MHz; DMSO-*d6*: 6.94 (dd, *J1*=7.6 Hz, *J2*=13.2 Hz, 2H, ArH), 7.28-7.32 (t, 1H, ArH), 7.85-7.87 (d, 1H, *J*=6.82 Hz, ArH), 8.05-8.07 (d, 1H, J=8.0 Hz, ArH), 8.37-8.39 (d, 1H, J=8.0 Hz, ArH), 8.87-8.97 (t, 2H, ArH), 10.21 (S, 1H, ArH), 11.73 (S, 1H, NH, ArH) (Fig-A53). ^{13}C NMR (DMSO-*d6*): δ(ppm): 116.32, 116.64, 119.49, 120.07, 123.03, 126.41, 129.30, 129.72, 131.91, 136.78, 144.37, 146.55, 156.89 (Fig-A54). LCMS (ESI-MS) m/z: [M-H]$^-$ Calculated for $C_{13}H_{10}N_4O_5$, 302.07, Found: 302.95 (Fig-A52). FT-IR (KBr) ν (cm-1) = 3269, 3103, 1514, 1583, 1510, 1417, 1332, 1313, 1217, 1199, 1134, 1085, 962, 920, 821, 754, 715, 678, 648, 611, 528 (Fig-A51). Yield=81%.

2.2. UV-visible study of the receptor (S1-S4) with anions

For UV-Visible spectroscopic experiments of receptor (S1-S4) concentration (2.0×10^{-5} M) was prepared and different anion selectivity was investigated by the addition of different

ACCEPTED MANUSCRIPT

equivalents of various anions (1.0×10^{-2} M) independently to (2.0×10^{-5} M) stock solutions (S1-S4) in organic (DMSO) and organo-aqueous (DMSO: H_2O, 9:1) medium and analyzed their absorbance values from 250 to 700 nm. UV-visible titration experiments were recorded by continues addition of different equivalents of the various anions through a micropipette added to a 2ml (2.0×10^{-5} M) solution (S1-S4) in a cuvette in organic (DMSO) and organo-aqueous (DMSO: H_2O, 9:1) medium and the absorption spectra were recorded[43].

2.2 NMR titration experiments

The proceeding results of ^{1}H NMR titration studies determined the sensing of fluoride and cyanide ions by S1 receptors through the development of receptor-fluoride and cyanide ion complex. In order to confirm the mechanism of sensing, ^{1}H NMR titration study was performed with the receptor S1 in DMSO-*d6* by the addition of 0.5, 1.0 and 1.5 equivalents of fluoride and cyanide ions and the ^{1}H NMR titration spectra were shown in Fig-12 and Fig-13.

2.3 Density functional theory calculations

The quantum chemical calculations of the density functional theory on the aromatic aldehyde receptor were performed to support analyzing the optical behavior and method of complexation of the aromatic aldehyde receptor with fluoride and cyanide ions. The geometry optimizations and frontier molecular orbital properties of the molecule at DMSO solvent phase performed by density functional theory with B3LYP exchange with 6-311G basics sets applying Maestro-MS.

3.0 Results and Discussion

3.1 Synthesis

As shown in scheme 1. the receptors S1, S2, S3 and S4 were designed and synthesized by a simple condensation reaction, by reacting 2,4 dinitrophenylhydrazine (0.430 g, 3 mmol) with cinnamaldehyde (0.594 g, 3 mmol) receptor S1, pyridine 3-aldehyde (0.321 g,3 mmol) receptor S2, 5-bromoalicyaldehdye (0.603 g,3 mmol), receptor S3 and salicylaldehyde (0.366 g,3 mmol) receptor S4, in ethanol (20ml) respectively. The reaction mixture was stirred at room

ACCEPTED MANUSCRIPT

temperature for 12 hours. After completion of the reaction, the obtained yellow precipitate was filtered and washed several times with ethanol to yield the pure receptors (S1-S4). The completion of the pure product was confirmed by thin layer chromatography (TLC). All the prepared simple Schiff bases (S1-S4) have been characterized by ^{13}C NMR, ^{1}H NMR, Mass spectra and IR analysis of spectroscopic methods.

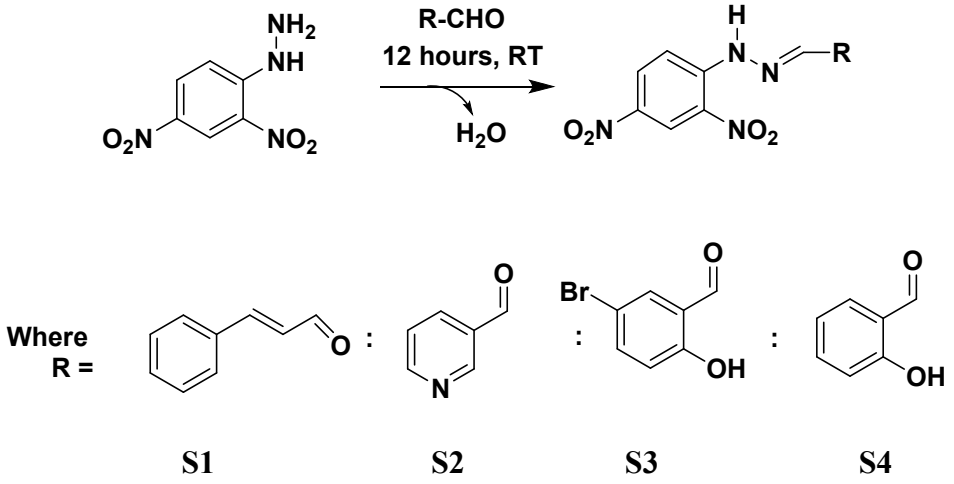

Scheme 1. Synthesis of receptor S1-S4.

3.2 Colorimetric detection of anions in organic and organo-aqueous medium

The naked eye response of receptor S1-S4 (2.0×10^{-5} M) against different anions such as F^-, Br^-, I^-, Cl^-, OH^-, HSO^-_4, NO^-_3, NO^-_2, F^- and CN^- (1.0×10^{-2} M) was first analyzed through colorimetric chemosensor analysis in organic (DMSO) medium. It was established that among the receptors S1-S4, only S1 displayed a drastic color change from yellow to purple with fluoride and cyanide ions showed in Fig-A1 (information from ESI*), where as receptors S2-S4 displayed a visual color change from pale yellow to pink with fluoride and cyanide ions showed in Fig-A6, A24, A42 (information from ESI*). No significant color changes of other anions such as Br^-, I^-, Cl^-, OH^-, HSO^-_4, NO^-_3 and NO^-_2 ions under same conditions were noticed as shown in Fig-1 and those related to receptors S2-S4 are showed in Fig-A8, A26, A44 (information from

ESI*). Receptor S1 colorimetric chemosensor analysis was also carried out in organo-aqueous medium (DMSO: H_2O, 9:1). It exhibited an optical color change from pale yellow to pink only with fluoride and cyanide ions showed in Fig-A6, A24, A42 (information from ESI*), while no visual response was observed on other anions such as Br^-, I^-, Cl^-, OH^-, HSO^-_4, NO^-_3 and NO^-_2 ions as shown in Fig-2 and related receptor of S2-S4 showed in Fig-A8, A26, A44 (information from ESI*).

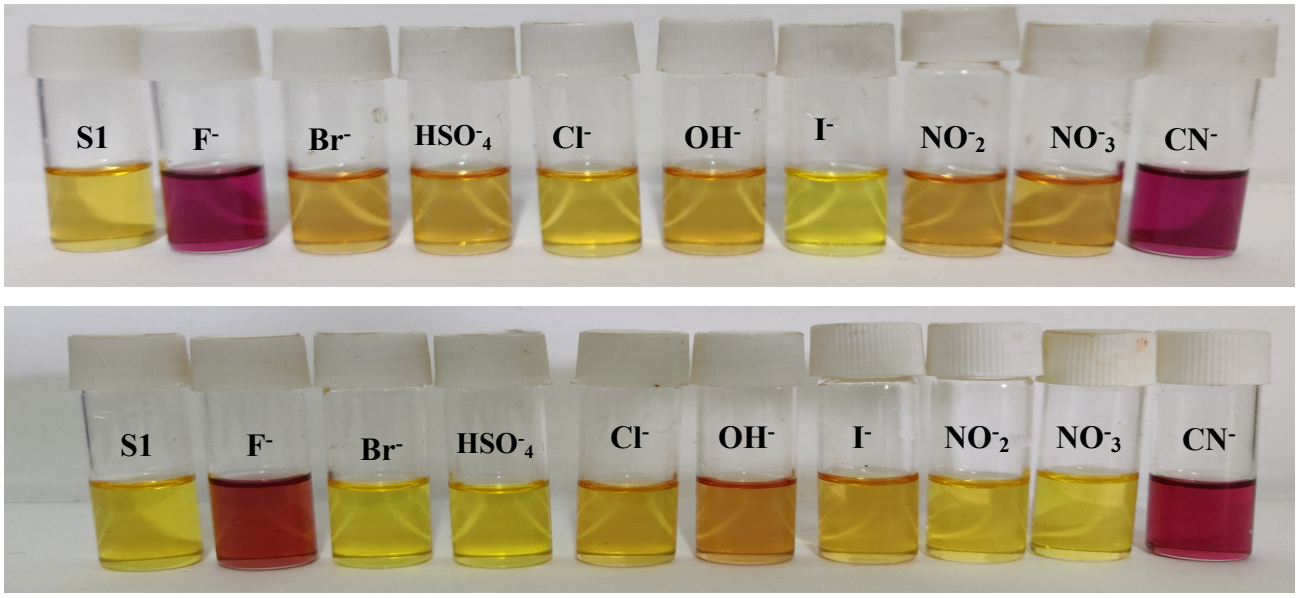

Fig-1&2. Visual color change of receptor S1 (2.0×10^{-5} M in dry DMSO) after the addition of 3.3 equivalent and S1 (2.0×10^{-5} M in DMSO: H_20, 9:1) with the addition of 4.5 equivalent of different TBAF salts of anions (1×10^{-2} M).

3.3 UV-Visible spectroscopic titration of receptor S1 with Fluoride and Cyanide ions in DMSO

The visual interactions of receptor S1-S4 with fluoride and cyanide anions were measured by UV-Visible spectroscopic absorption technique. The UV-Visible absorption spectral changes of S1 upon the addition of fluoride and cyanide ions over the other anions are shown in Fig-3 and those related to receptors S2-S4 were shown in Fig-A7, A25, A43 (information from ESI*). The UV-Visible spectrum of receptor S1 advertised a maximum absorbance at 406 nm molar absorption coefficient logε = 5.83 which corresponds to the intermolecular charge transfer (ICT) transition (n-π*) from N-atoms to the aldehyde moiety as

ACCEPTED MANUSCRIPT

shown in Fig-3, on the addition of fluoride (0.0-3.3 equivalents) and cyanide (0.0-3.75 equivalents) the visual color of receptor changed from pale yellow to purple showed in Fig-A1 (information from ESI*) and other receptors S2-S4 showed drastic color changes from pale yellow to pink showed in Fig-A6, A24, A42 (information from ESI*).

A new peak was developed at 517 nm and 515 nm resulting from the complex between receptor S1 with fluoride and cyanide ions. It indicated the bathochromic shifts of λ_{ICT}= 111 nm and 109 nm (Fig-3). In this case N-H····F^- and N-H····CN^- is a relatively good electron donor than free N-H in the intermolecular charge transfer (ICT) transition in receptor S1[44-46], while the fluoride and cyanide ions were bound *via* H-bonding interaction from the amine group of receptor S1, the electron cloud density of electron rich amine fragment was further increased which developed the charge transfer interaction between electron rich and electron deficient DNP moiety.

The UV-Visible titration, of receptor S1 was carried out in DMSO medium by taking different equivalent of F^- (0.0-3.3 equivalent) and CN^- (0.0-3.75 equivalent). Upon addition of fluoride and cyanide ions, the absorption peak at 402 nm was shifted to 517 nm which was attributed to the charge transfer between F^- and CN^- with high acidic –NH unit of the receptor S1 (Fig-3)[47-49]. The final colorimetric UV-Visible titration confessed a clear isosbestic point of 452 nm which determined the formation of a strong complex between receptor S1 with F^- and CN^-. Absorption spectra of S1 (2.0×10^{-5} M) in the presence of fluoride ion (up to 3.3 equivalent of TBA-F) and cyanide ion (up to 3.75 equivalent of TBA-CN) in DMSO showed in Fig-9. All other receptors S2-S4 produced a comparable UV-Visible spectral changes with fluoride and cyanide showed in Fig-A9, A27, A45 (information from ESI*). Extended variation method was used to determine the stoichiometric ratio of the receptor, fluoride and cyanide ions guest. In Fig-11, Job's plot of receptor S1 (1×10^{-4} M) with F^- and CN^- in DMSO medium shows a maximum at a mole fraction of 0.5. These results were shows that the receptor S1 binds with fluoride and cyanide anion with a 1:1 stoichiometric ratio to form complex and receptor S2-S4 showed in Fig-A14, A32, A50 (information from ESI*).

ACCEPTED MANUSCRIPT

3.4 UV-Visible spectroscopic titration of receptor S1 with Fluoride and Cyanide ions in Organo-aqueous medium

The sensing capacity of the receptor S1 was carried out in DMSO: H_2O (9:1, V/V) solution. The optical color changes were seen for F^- and CN^- ions on binding with receptor S1 even in existence of protic solvent of H_2O as shown in Fig-6. The protic solvent of H_2O contest with anion binding sites of the receptor nearby annoying the cooperation between receptor and anion. However, the receptor S1 demonstrated the capability of water molecules to bind with anions in aqueous medium and recommended the hydrogen-bond interaction between anions and receptor S1. UV-Visible spectrum was recorded on stepwise addition up to 5.0 equivalent of F^- and 5.25 equivalent of CN^- ions in the DMSO: H_2O (9:1, V/V). The solution displayed changes in UV-Visible absorbance spectrum from F^- and CN^- ions shown in Fig-6 and other receptors S2-S4 showed in Fig-A7, A25, A43 (information from ESI*). The stepwise addition of 0.0-5.0 equivalents of F^- ions (1×10^{-2} M) to the receptor (2.0×10^{-5} M) increases its absorbance band from 405 nm to 512 nm with sharp isosbestic point of 449 nm, showing regular interaction with receptor S1 and F^- ions with a bathochromic red shift of 107 nm and with drastic color changes from pale yellow to pink showed in Fig-A14, A32, A50 (information from ESI*). On the other hand incremental addition of 0.0-5.25 equivalents of CN^- ions to the DMSO: H_2O (9:1, V/V) (2.0×10^{-5} M) displayed new absorbance band at 509 nm, resulting in bathochromic shift of 104 nm with the isosbestic point at 449 nm which convey that a new species is formed in response to the interaction with receptor S1 and anions shown in Fig-6.

When similar set of UV-Visible spectroscopic titration was carried in organo-aqueous medium (DMSO: H_2O, 9:1, V/V), it was interesting to observe that, the receptor S1 advertised a drastic color changes from pale yellow to pink only with fluoride and cyanide ion while no color change was observed with Br^-, I^-, Cl^-, OH^-, HSO^-_4, NO^-_3 and NO^-_2 ions shown in Fig-10.

3.5 Determination of stoichiometry, binding constant, the limit of detection and limit of quantification

Bensi-Hilderbrand (B-H) plot was sketched between 1/(A-A0) and $1/[Mn+]^2$ according to the B-H equation 1. The receptor S1 upon incremental addition of the F^- and CN^- showed 1:2 binding stoichiometric ratio in DMSO and DMSO: H_2O, 9;1 shown in Fig-5 & Fig-8 and related receptor S2-S4 showed in Fig-A12, A13, A30, A31, A48, A49 (information from ESI*). The

ACCEPTED MANUSCRIPT

binding constant between receptor S1-F^- and CN^- were calculated and given in the table below Table 2.

Linearity plotted between absorbance v/s concentration of F^- and CN^- in molar shown in Fig-4 & Fig-7 and remaining receptor S2-S4 showed in Fig-A10, A11, A28, A29, A46, A47 (information from ESI*). A good relationship between absorbance and concentration with the R^2>0.99. The limit of detection & limit of quantification was calculated using the equation given bellow and showing in Table 2.

Equation 1. $$K = \frac{A - A_0}{A_{max} - A} \times \frac{1}{[Mn+]n}$$

Where

K = is the association constant

A_0= is the absorbance of receptor in the absence of guest.

A = is the absorbance recorded in the presence of an added guest.

Amax = is absorbance in the presence of added [Mn+]max.

[Mn+] n = concentration of fluoride and cyanide ion with binding ratio.

Limit of Detection = 3.3* Standard deviation of calibration curve (SD) / Slope.

Limit of quantification = 10* Standard deviation of calibration curve (SD) / Slope.

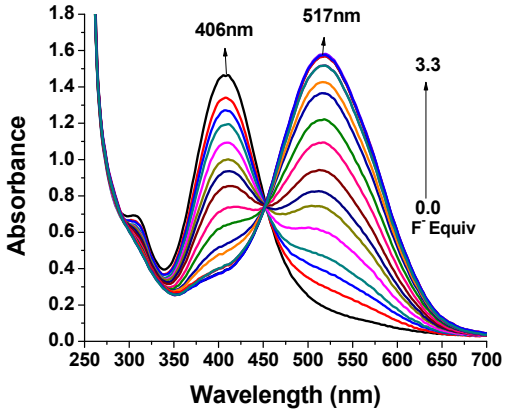

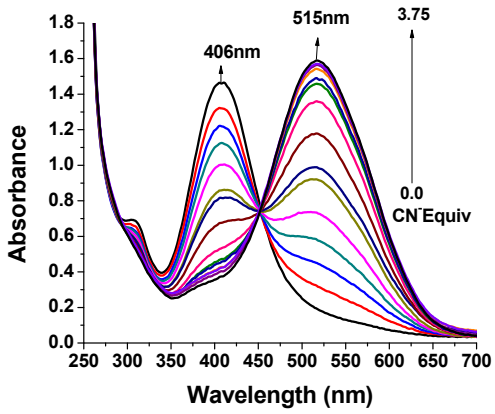

ACCEPTED MANUSCRIPT

Fig-3. UV-Visible absorption changes of receptor S1 (2.0×10^{-5} M) upon addition of (0.0 to 3.3 equivalent) of TBA-F and (0.0 to 3.75 equivalent) of TBA-CN (1.0×10^{-2} M) in DMSO.

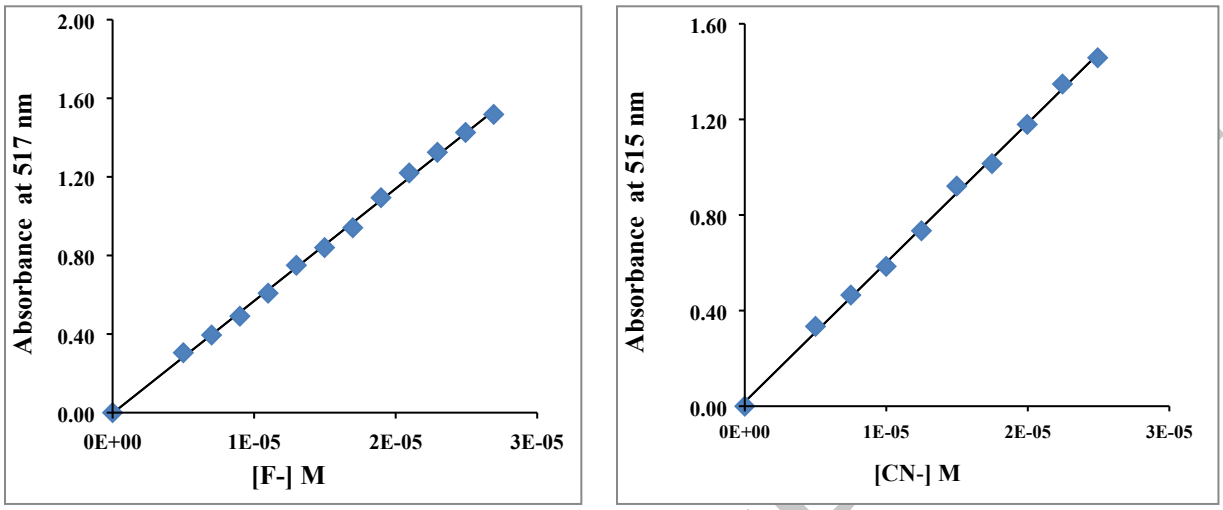

Fig-4. Calibration curve for the determination of detection limit of receptor **S1** with Fluoride and Cyanide ions in DMSO.

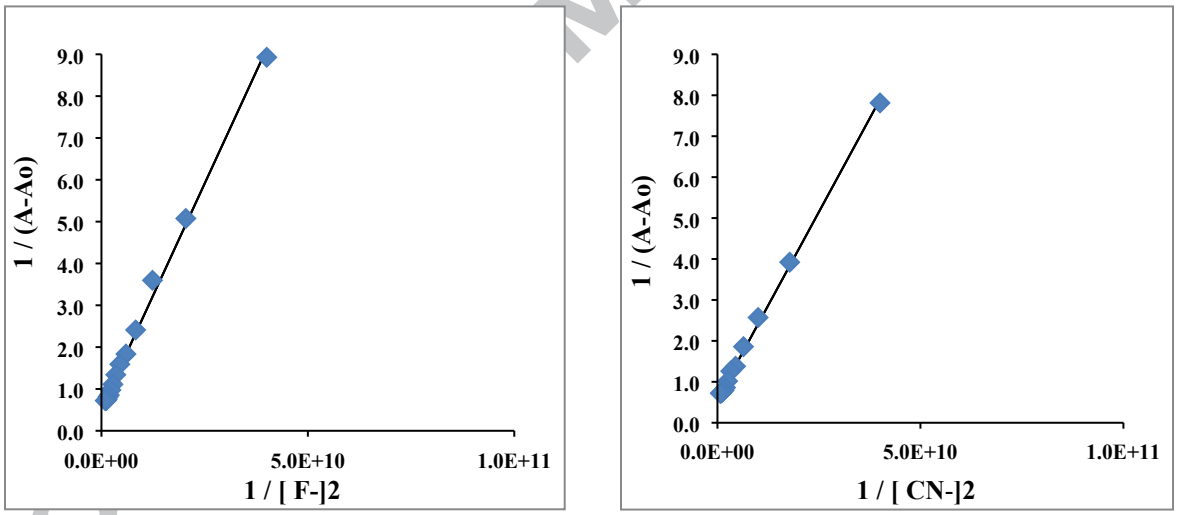

Fig-5. Inset: B–H plot for the titration of receptor S1 with F^- and CN^- ion in DMSO.

ACCEPTED MANUSCRIPT

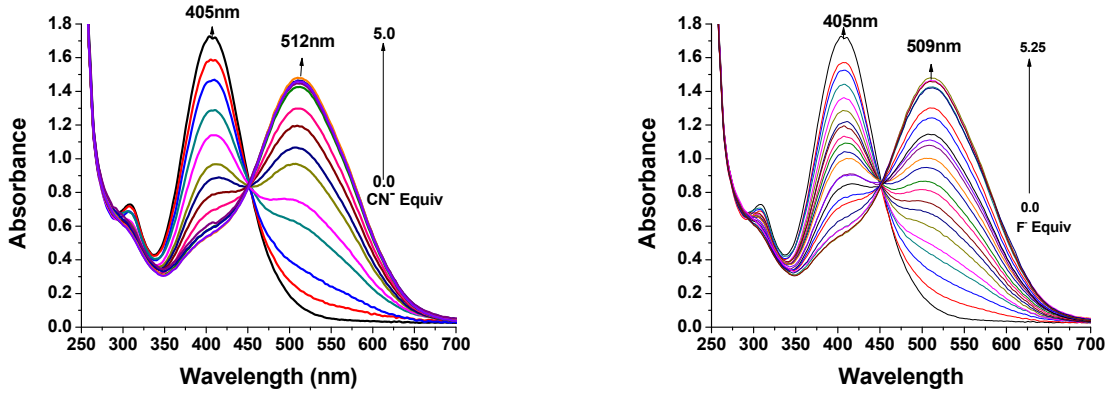

Fig-6. UV-Visible absorption changes of receptor S1 (2.0×10^{-5} M) upon addition of (0.0-5.0 equivalent) of TBA-F and (0.0 to 5.25 equivalent) of TBA-CN (1.0×10^{-2} M) in DMSO: H_2O (9:1).

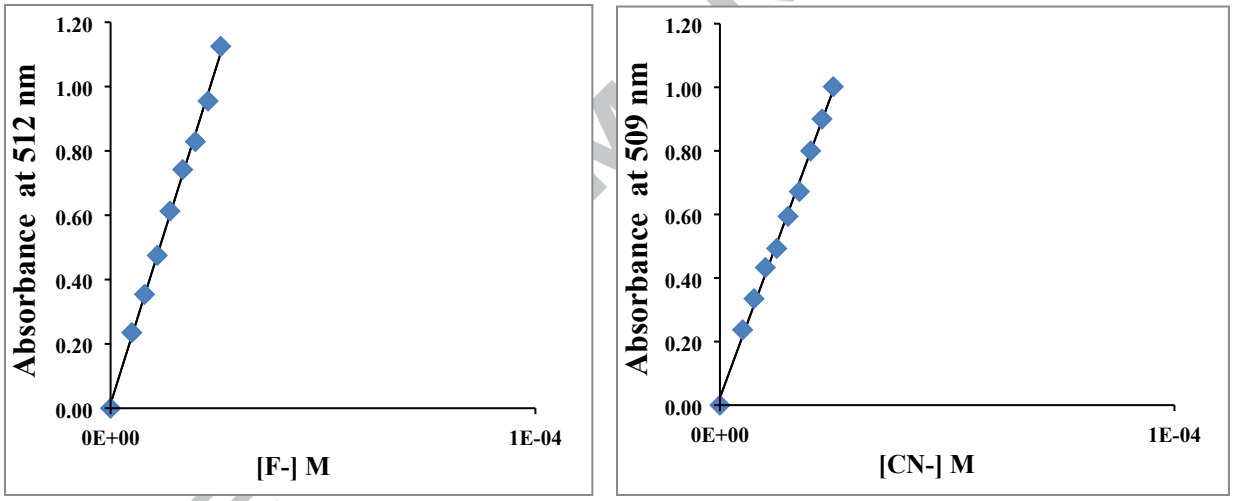

Fig-7. Calibration curve for the determination of detection limit of receptor S1 with fluoride and cyanide ion in DMSO: H_2O (9:1, v/v).

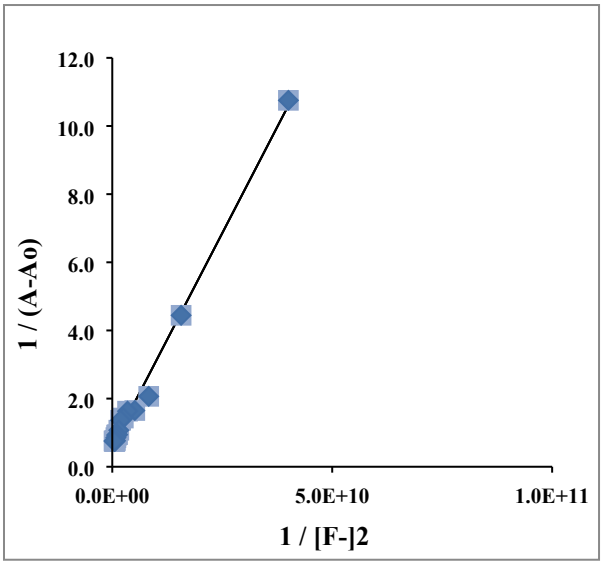

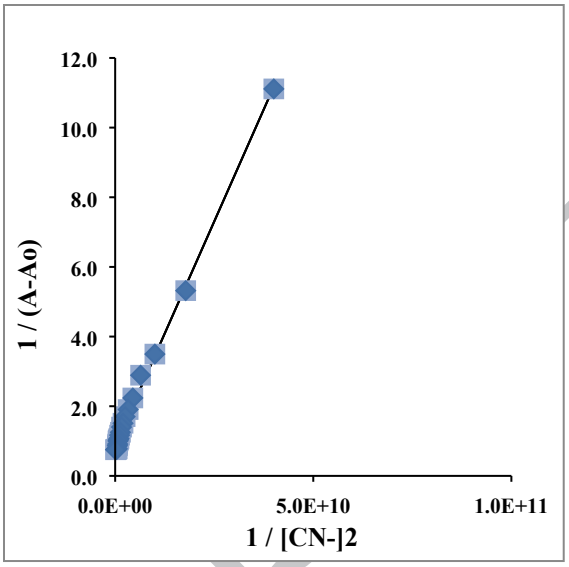

Fig-8. Inset: B–H plot for the titration of receptor S1 with F^- and CN^- ion in DMSO: H_2O (9:1).

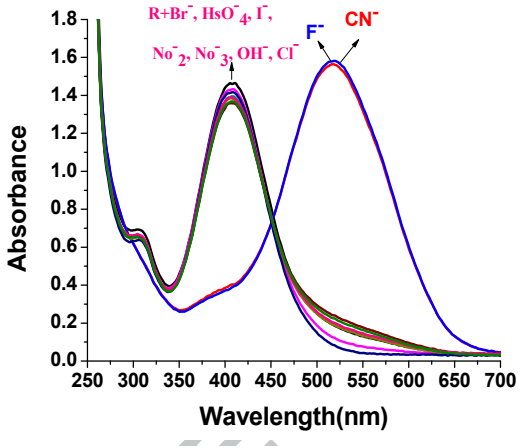

Fig-9. UV-Visible Absorption spectra of receptor S1 (2.0×10^{-5} M) in the absence and presence of different anions (3.3 equivalent of TBA-F and 3.75 equivalent of TBACN (1.0×10^{-2}

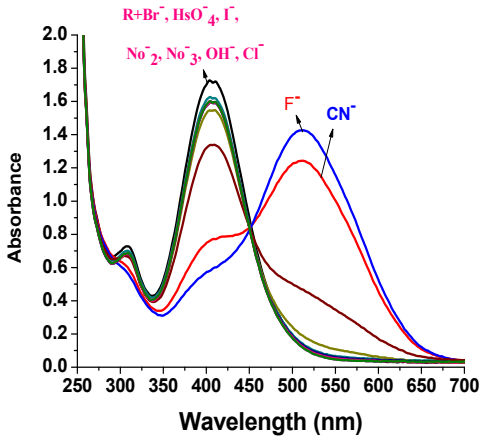

Fig-10. UV-Visible absorption changes receptor S1 (2.0×10^{-5} M) upon addition of (5.0 equivalent) of TBAF and (0.0 to 5.25 equivalent) of TBACN (1.0×10^{-2} M) in DMSO: H_2O (9:1).

ACCEPTED MANUSCRIPT

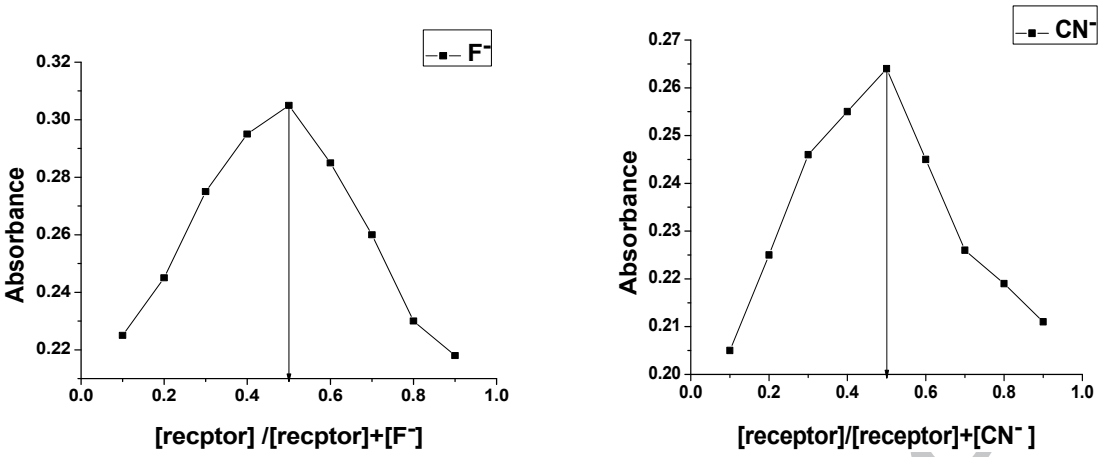

Fig-11. Job's plot for complexation of receptor S1 (517 nm) and (515 nm) with F^- and CN^- ions determined by UV-visible experiments in (DMSO) organic medium.

Table1. Selected absorption spectra of receptors S1-S4 (2.0×10^{-5} M) in DMSO and DMSO: H_2O (9:1, V/V) medium in the presence of F^- and CN^- ions (1.0×10^{-2} M) in different equivalent

Receptor	Medium of Detection	UV-Visible band in nm without F^- and CN^-	UV-Visible band in nm with F^- ion	UV-Visible band in nm with CN^- ion	Bathochromic Shift in visible band in nm F^-&CN^-	Visible color change
S1	DMSO	406	517	515	111 &109	Pale yellow to purple
S2	DMSO	390	504	502	114 &112	Pale yellow to pink
S3	DMSO	404	508	506	102 &104	Pale yellow to pink
S4	DMSO	405	499	497	94 &92	Pale yellow to pink
S1	DMSO:H_2O (9:1.V/V)	405	512	509	107&104	Pale yellow to pink
S2	DMSO: H_2O (9:1.V/V)	389	499	498	110&109	Pale yellow to pink

ACCEPTED MANUSCRIPT

S3	DMSO: H_2O (9:1.V/V)	406	502	503	97&96	Pale yellow to pink
S4	DMSO: H_2O (9:1.V/V)	403	493	492	90&89	Pale yellow to pink

Table 2. Association constant and Binding constant, Limit of Detection and Limit of Quantification of receptor S1-S4 in the presence of fluoride and cyanide ions.

R+Anions	Association constant M^{-1}	Binding constant in M^{-1}	LOD in ppm	LOQ in ppm
S1+TBAF(DMSO)	2.1×10^5	2.58×10^9	0.268	0.8
S1+TBACN(DMSO)	2.9×10^5	3.19×10^9	0.314	1.0
S2+TBAF(DMSO)	1.0×10^5	3.4×10^9	0.258	0.80
S2+TBACN(DMSO)	1.0×10^4	1.59×10^9	0.292	0.90
S3+TBAF(DMSO)	8.7×10^4	1.2×10^9	0.60	0.55
S3+TBACN(DMSO)	2.9×10^5	7.6×10^8	0.20	0.18
S4+TBAF(DMSO)	1.1×10^5	4.0×10^9	0.20	0.60
S4+TBACN(DMSO)	1.8×10^5	1.02×10^9	0.10	0.30
S1+TBAF(DMSO:H_2O, 9:1)	7.4×10^4	2.49×10^9	0.12	0.40
S1+TBACN(DMSO:H_2O, 9:1)	3.0×10^4	3.75×10^9	0.19	0.60
S2+TBAF(DMSO:H_2O, 9:1)	1.6×10^5	1.69×10^9	0.230	0.70
S2+TBACN(DMSO:H_2O, 9:1)	2.9×10^4	5.61×10^9	0.33	1.0
S3+TBAF(DMSO:H_2O, 9:1)	3.7×10^5	7.0×10^9	0.27	0.80
S3+TBACN(DMSO:H_2O, 9:1)	2.5×10^5	3.8×10^9	0.5	0.15
S3+TBAF(DMSO:H_2O, 9:1)	1.9×10^5	4.73×10^9	0.558	1.70
S3+TBACN(DMSO:H_2O, 9:1)	1.1×10^5	5.33×10^9	0.451	1.40

ACCEPTED MANUSCRIPT

3.6 [1]H NMR titration study of receptor S1 with Fluoride and Cyanide ions

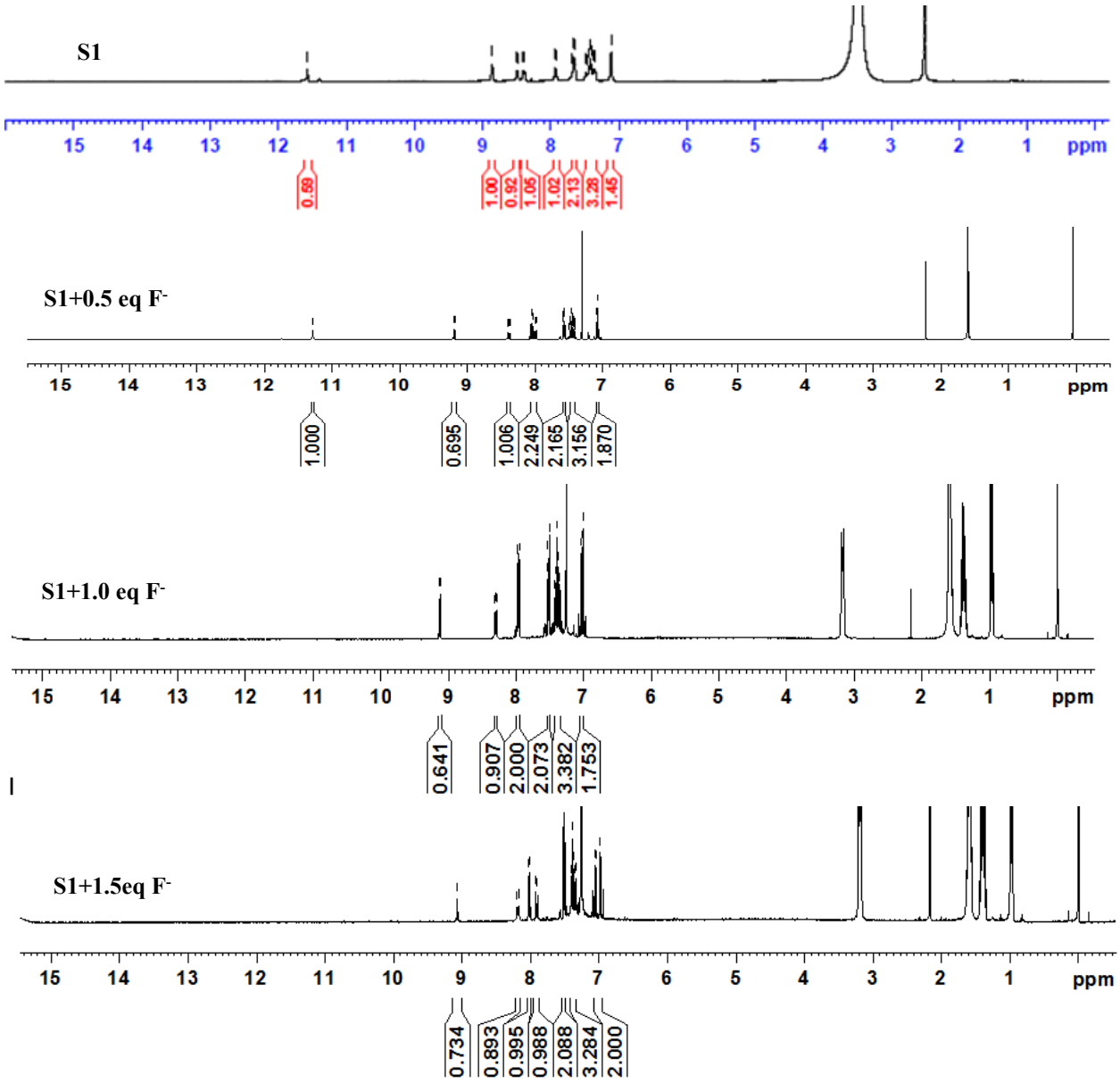

Fig-12. Titration of S1 with TBA-F in DMSO-d6 as monitored by [1]H NMR spectroscopy.

ACCEPTED MANUSCRIPT

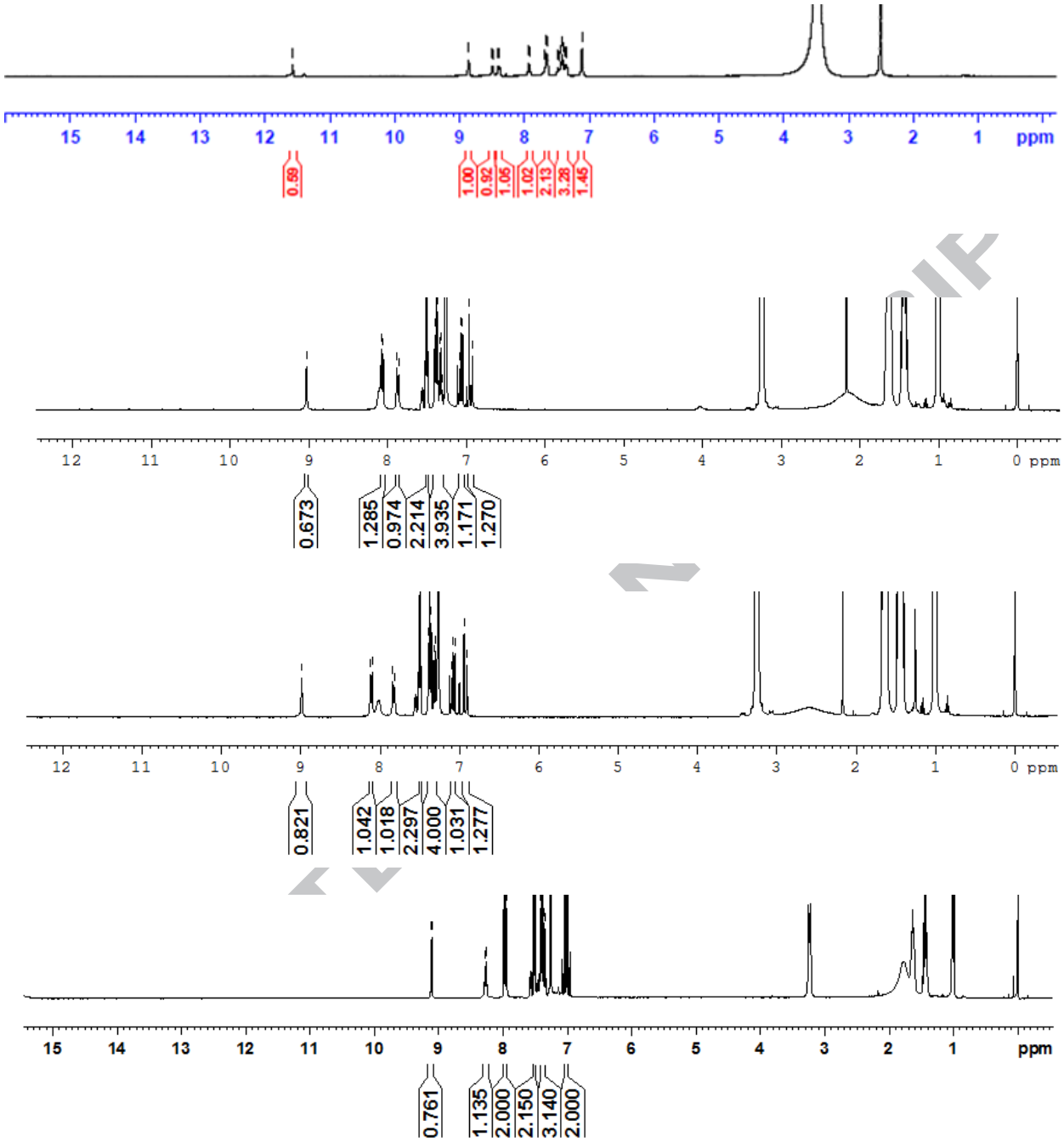

Fig-13. Titration of S1 with TBA-CN in DMSO-d6 as monitored by ^{1}H NMR spectroscopy.

The chemosensor property exhibited by the receptor S1 was observed by UV-visible spectroscopy. In order to analyze the sensing mechanism of the receptor S1 with fluoride and cyanide, the ^{1}H NMR titration study was investigated shown in Fig-A12 and Fig-A13. In 2,4 dinitrophenylhydrazine the signal corresponds to –NH proton was observed at 8.85 ppm, when

ACCEPTED MANUSCRIPT

the 2,4 DNP attached with aromatic aldehyde the signal was observed at 11.56 ppm in the presence of N-H proton. This is due to the existence of ICT between 2,4 DNP and aromatic aldehyde. ^{1}H NMR titration of receptor S1 observed with tetrabutylammonium fluoride and cyanide ion in DMSO-*d6*. The addition of 0.5 equivalent of fluoride the comparable (11.26 ppm) –NH proton peak was shifted to slightly up field and the addition of 1.0, 1.5 equivalent of fluoride resulted, disappeared –NH proton in the ^{1}H NMR spectra. On the other hand, the receptor S1 complex with CN^- in ^{1}H NMR titration, the addition of 0.5, 1.0 and 1.5 equivalent of CN^- the corresponding (11.56 ppm)–NH proton had completely disappeared. The mechanism is that –NH proton moiety of the receptor S1 interacts with F^- and CN^- through hydrogen bonding and formed by the more F^- and CN^- in the interaction inducing proton transfer reaction and density of the electron increased shown in scheme 2.

This leads to ICT in the whole system and red shift in the absorption on the addition of F^- and CN^-. At the meantime, the electron density of nitro aromatic aldehyde ring was gradually increased and the hydrogens of aromatic ring shifted upfield automatically. Therefore, color change can be showing to the formation of hydrogen bonding between –NH moiety and F^-, CN^- ions.

ACCEPTED MANUSCRIPT

ACCEPTED MANUSCRIPT

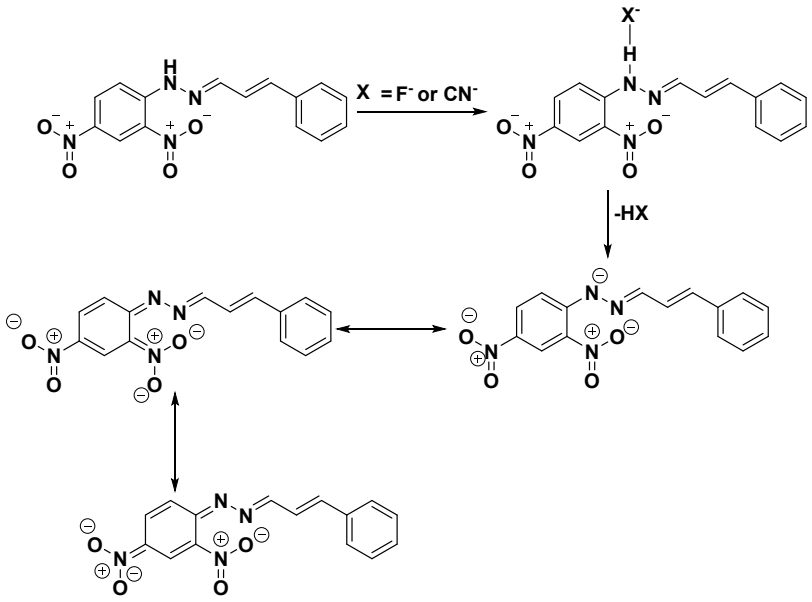

Scheme 2. Interaction of fluoride respectively cyanide anions with the receptor S1 including mesomeric formulae of deprotonated S1.

3.7 Computational study of receptor S1-S4 with fluoride and cyanide ion.

To understand the photophysical properties of the receptors S1-S4 and its calculation with fluoride and cyanide ions were carried out by theoretical methods using Maestro-MS calculation. The receptor (S1-S4) were optimized and complexes with the electronic ground and excited state through Density Functional Theory (DFT) calculation using the B3LYP/6-311G basis set with the fluoride and cyanide ions observed by using Maestro-MS software (Fig-14).

The additional information about the mechanism of interaction between S1 complexes with anions was obtained from the typical transition energy diagram for the HOMO and LUMO of the receptor S1 with its complex with fluoride and cyanide ions as shown in Fig-14 and related receptor S2-S4 showed in Fig-A19, A37, A55 (information from ESI*). The more disturbed HOMO layer with DNP moieties and also the distribution of aldehyde moiety. On the deprotonated species, mostly HOMO layer was located with aldehyde moieties and LUMO was distributed in aldehyde and DNP moieties. Therefore, binding of fluoride and cyanide with receptor S1 and the electron density through extended JI-conjugation, which leads to the homogenous distribution throughout the molecule. The aspect had been well explained in the ICT [50-51].

The bathochromic shift of the absorption band of receptor S1 when binding with fluoride and cyanide ions might be further understood in terms of increase of the potential energy of its HOMO & LUMO shown in Fig-14. The energy gap between HOMO and LUMO of receptor S1 decreased on its binding with fluoride and cyanide. The fluoride and cyanide ions would prefer electron deficient LUMO more rather than HOMO. Therefore, on binding with fluoride and cyanide the potential energy of the LUMO slightly decreased moderately and finally directed towards the narrowing of the energy gap between HOMO &LUMO, which was ultimately responsible for the red shift of absorption maximum of receptor S1 complex with fluoride and cyanide.

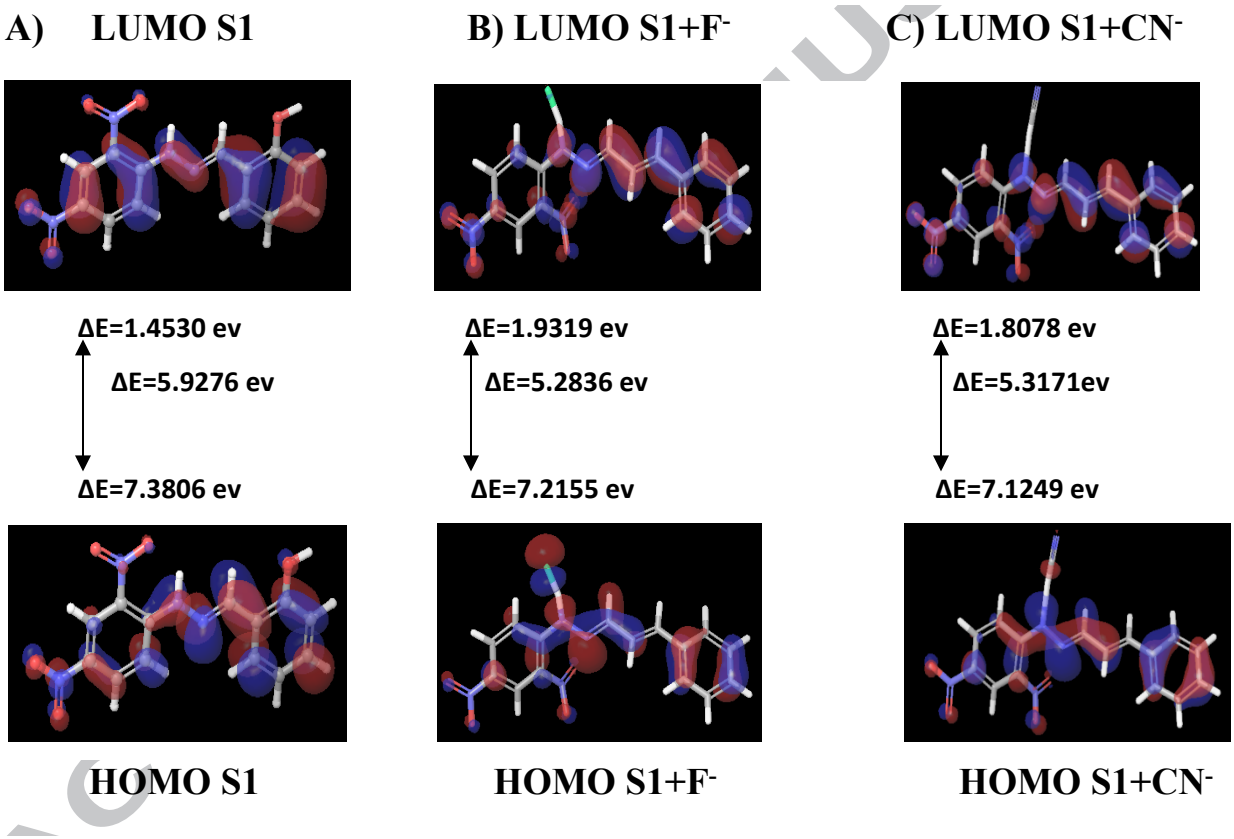

Fig-14. HOMO'S and LUMO'S diagrams for (A) receptor S1, (B)receptor S1+F^-, (C) receptor S1+CN^- obtained by the B3LYP/6-311G method.

ACCEPTED MANUSCRIPT

3.8 Practical applications in real sample analysis of Receptor S1

Further study, practical applications in real sample analysis of receptor S1 was carried out by qualitative determination of fluoride and cyanide ions in commercially usable products such as toothpaste and mouthwash. Mouthwash & toothpaste sample was weighed 20 mg in 1ml by dissolving distilled water[52]. Finally, a drop of commercially useable mouthwash and toothpaste was added into the receptor S1, a drastic color change from pale yellow to A) orange & B) pink correlation as shown in Fig-15. The UV-visible absorption spectra recorded with receptor S1 in the presence of mouthwash and toothpaste showing similar charge transfer absorption band as observed in the case of fluoride and cyanide ions are shown in the Fig- 15. All other receptors (S2-S4) analysis showed in Fig-A20, A21, A38, A39, A56, and A57 (information from ESI*).

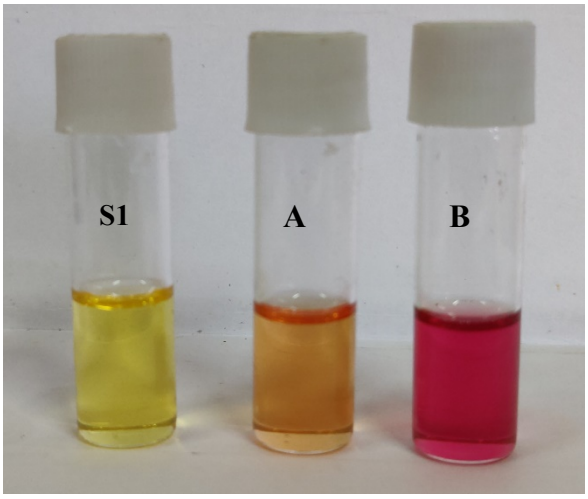

Fig-15. The color change of the receptor S1 (2.0×10^{-5}M) upon addition of a drop of (A) mouthwash and (B) toothpaste.

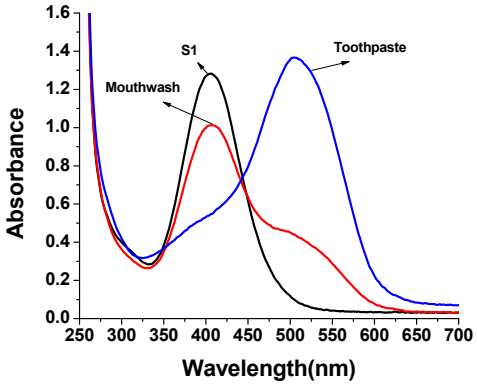

Fig-16. Absorption spectra of receptor S1 (2.0×10^{-5} M) upon addition of a drop of mouthwash and toothpaste.

ACCEPTED MANUSCRIPT

3.9 Practical application

In the present investigation of receptor S1, test strips were prepared by using Whatman-40 test paper immersing into DMSO solution and dried in the hot air oven. Upon this light-yellow colored strip was observed and which was then dipped into an aqueous solution of (A) TBA-F and TBA-CN of different concentration shown in Fig-17 and Fig-18, receptor S2-S4 showed in Fig-A22, A23, A40, A41, A58, A59 (information from ESI*), this showed drastic color changes. Finally, we concluded this kind of application is more efficient and less expensive, new receptor will be more advantageous in sensing of these anions in real life application.

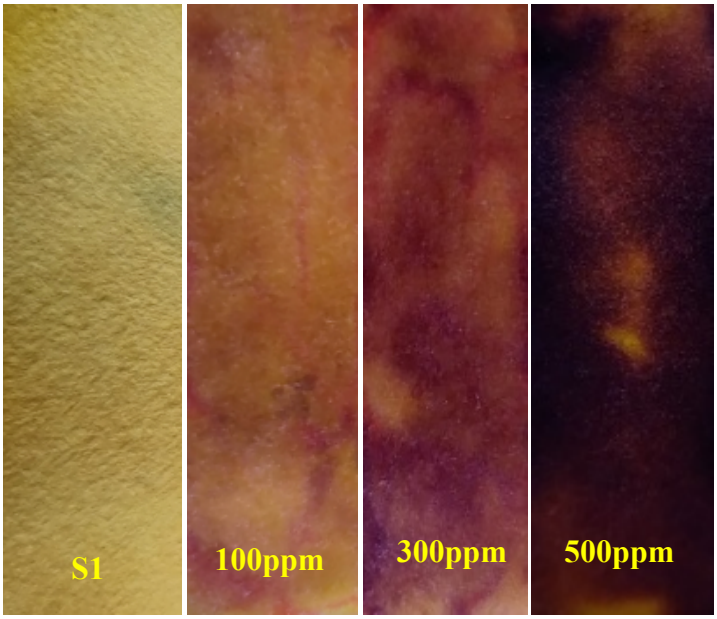

Fig-17. Color changes of test papers prepared using receptor S1 for detecting F^- ions in aqueous solution with different concentration.

ACCEPTED MANUSCRIPT

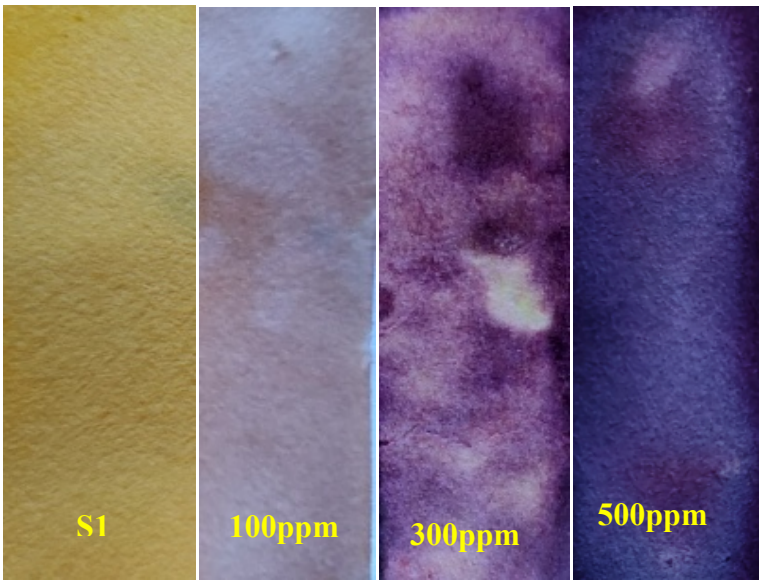

Fig-18. Color changes of test papers prepared using receptor S1 for detecting CN^- ion in aqueous solution with different concentration.

Conclusion

To illustrate, the simple and efficient colorimetric sensors, receptor S1-S5 based on aromatic aldehyde with –NH as a hydrogen donor. To analyze the UV-visible absorption spectroscopy of receptor (S1-S4) showing higher selectivity for fluoride and cyanide ions without any distinct color from other anions, the bathochromic shift was observed on maximum absorption. The receptor S1 shows a dramatic color change from pale yellow to purple and (S2-S4) pink upon addition of fluoride and cyanide in DMSO medium and S1-S4 shows drastic color change from yellow to pink in organo-aqueous (DMSO: H_2O, 9:1) medium. ^1H NMR titration can be done the reaction between receptor S1-S4 with fluoride and cyanide which indicate the delocalization of electron in the system and intermolecular charge transfer would increase exhibiting UV-Visible absorption spectra red shift significantly. Finally, the quantum mechanical calculation through DFT well supported the experimental findings.

ACCEPTED MANUSCRIPT

Acknowledgement

One of the authors would like to thank Mangalore University for providing research fellowship. Authors gratefully acknowledge SAIF, IISC Bangalore for providing NMR characterization and DST-PURSE, Mangalore University for providing characterization facilities.

ACCEPTED MANUSCRIPT

Reference.

[1] N. Chen, Z. Zhang, C. Feng, D. Zhu, Y. Yang, N. Sugiura, J. *Hazard. Mater*. 186 (2011) 863–868.

[2] WHO, Guidelines for Drinking Water Quality Incorporating 1st and 2nd Addenda Recommendations, third ed, World Health Organization, Geneva, Switzerland. 2008.

[3] X. Xiong, J. Liu, W. He, T. Xia, P. He, X. Chen, K. Yang, A. Wang, *Environ. Res*. 103 (2007) 112–116.

[4] Jung Oh Huh, Youngkyu Do, and Min Hyung Lee. *Organometallics*. 27 (2008) 1022–1025.

[5] Ki. Cheol Song, Kang Mun Lee, Nguyen Van Nghia, Woo Young Sung, Youngkyu Do, and Min Hyung Lee. *Organometallics*. 32 (2013) 817−823.

[6] Syed S. Razi, Rashid Ali, Priyanka Srivastava, Arvind Misra, *Tetrahedron Letters.* 55 (2014) 1052–1056.

[7] K.W. Kulig, Cyanide Toxicity, U. S. Department of Health and Human Services, Atlanta, GA, 1991.

[8] A. Dhillon, M. Nairb, D. Kumar, Analytical methods for determination and sensing of fluoride in biotic and abiotic sources: a review, *Anal. Methods*. 8 (2016) 5338-5352.

[9] Todd W. Hundnall, Ching-Wen Chiu. 42,2 (2009) 388-397.

[10] Stephen J. Butler. *Chem. Commun*. 51 (2015) 10879-10882.

[11] Muhammad Moazzam Naseera, b and Klaus Jurkschata, *Chem. Commun*.53 (2017) 8122–8135.

[12] Sudeshna Chandra, Ales Ruziicka, Petr Svec, Heinrich Lang *Analytica Chimica Acta*. 577 (2006) 91–97.

[13] George Rajendra Kumar and Pakkirisamy Thilagar. *Dalton Trans*. 43 (2014)7200-7207.

[14] Youngmin Kim, Hyun-Sue Huh, Min Hyung Lee, Ivan L. Lenov, Haiyan Zhao, and FranÅois P. Gabba, *Chem. Eur. J*. 17 (2011) 2057 – 2062.

[15] Kirk, K. L. Biochemistry of the Halogens and Inorganic Halides; Plenum Press: New York. (1991) 58.

[16] Kleerekoper, M. Endocrinol. Metab. *Clin. North Am.* 27 (1998) 441.

[17] R. Vilar, Angew. *Chem. Int. Ed*. 42 (2003) 1460–1477.

[18] Y. M. Hijji, B. Barare, A.P. Kennedy, R. Butcher, Sens. Actuators B. 136 (2009) 297–302.

[19] Atsushi Kawachi, Atsushi Tani, Junpei Shimada, and Yohsuke Yamamoto. *J. Am. Chem. Soc*. 130 (2008) 4222-4223.

[20] Amos B. Smith, *Org. Lett.* 14 (2012) 1-2.

[21] J. Li, H. Lin, Z. Cai, H. Lin, *Spectrochim. Acta A*. 72 (2009) 1062–1065.

[22] G.V. Zyryanov, M. A. Palacios, J. P. Anzenbacher, Angew. *Chem. Int. Ed*. 46 (2007) 1.

[23] T. P. Lin, C.Y. Chen, Y.S. Wen, S. S. Sun, *Inorg. Chem*. 46 (2007) 9201–9212.

[24] J. F. Zhang, C.S. Lim, S. Bhuniya, B.R. Cho, J.S. Kim, *Org. Lett*. 13 (2011) 1190–1193.

ACCEPTED MANUSCRIPT

[25] H. S. Jung, H. J. Kim, J. Vicens, J.S. Kim, *Tetrahedron Lett*. 50 (2009) 983–987.
[26] T. S. Snowden, E.V. Anslyn, Curr. Opin. *Chem. Biol*. 3 (1999) 740–746.
[27] M.Cametti, K. Rissanen, *Chem.Commun*. 20 (2009) 2809–2829.
[28] B. Liu, H. Tian, *J. Mater. Chem*. 15 (2005) 2681–2686.
[29] K. Chellappan, N. J. Singh, I. C. Hwang, J.W. Lee, K.S. Kim, Angew. *Chem. Int. Ed*. 44 (2005) 2899–2903.
[30] D. Esteban-Gomez, L. Fabbrizzi, M. Liechelli, *J. Org. Chem*. 70 (2005) 5717–5720.
[31] A.B. Descalzo, K. Rurack, H. Weisshoff, R. Martinez-Manez, M.D. Marcos, P. Amoros, K. Hoffmann, J. Soto, *J. Am. Chem. Soc.* 127 (2005) 184–200.
[32] D. A. Jose, D.K. Kumar, B. Ganguly, A. Das, *Tetrahedron Lett.* 46 (2005) 5343–5346.
[33] D. H. Lee, J.H. Im, J.H. Lee, J.I. Hong, *Tetrahedron Lett.* 43 (2002) 9637–9640.
[34] S. Devaraj, D. Saravanakumar, M. Kanadaswamy, *Tetrahedron Lett*. 48 (2007) 3077–3081.
[35] D. H. Lee, K.H. Lee, J.I. Hong, *Org. Lett.* 3 (2001) 5–8.
[36] X. Zhang, L. Guo, F.Y. Wu, Y.B. Jiang, *Org. Lett.* 5 (2003) 2667–2670.
[37] P. Anzenbacher, K. Jursikova, J. L. Sessler, *J. Am. Chem. Soc*. 122 (2000) 9350–9351.
[38] C. I. Lin, S. Selvi, J.M. Fang, P.T. Chou, C.H. Lai, Y.M. Cheng, *J. Org. Chem.* 72 (2007) 3537–3542.
[39] D. A. Jose, P. Kar, D. Koley, B. Ganguly, W. Thiel, H.N. Ghosh, A. Das, *Inorg. Chem*. 46 (2007) 5576-5584).
[40] Y. H. Qiao, H. Lin, H.K. Lin, J. Incl. Phenom. *Macrocycl. Chem*. 59 (2007) 211–215.
[41] R. L. Sheng, P.F. Wang, W.M. Liu, X.H. Wu, S.K. Wu, *Sens. Actuator B*. 128 (2008) 507– 511.
[42] Z. Lin, Y. Zhao, C. Duan, B. Zhang, Z. Bai, *Dalton Trans*. 30 (2006) 3678–3684.
[43] Archana Singh , Suban K. Sahoo , Darshak R. Trivedi. 188 (2018) 596-610.
[44] X.b Zhuang, W. Liu, J. Wu, H. Zhang, P. Wang, *Spectrochim. Acta A*. 79 (2011) 1352–1355.
[45] J. You, H. Jeong, H. Seo, S. Jeon, *Sens. Actuators B.* 146 (2010) 160–164.
[46] R. Vilar, Angew. *Chem. Int. Ed.* 42 (2003) 1460-1477.
[47] Y. M. Hijji, B. Barare, A.P. Kennedy, R. Butcher, *Sens. Actuators B.* 136 (2009) 297–302.
[48] J. Li, H. Lin, Z. Cai, H. Lin, *Spectrochemica. Acta A*. 72 (2009) 1062–1065.
[49] S. Saravana Kumar, S. Bothra, S.K. Sahoo, S.K. Ashok Kumar, *J. Fluorine Chem.* 164 (2014) 51-57.
[50] M.J. Frisch, G.W. Trucks, H.B. Schlegel, G.E. Scuseria, M.A. Robb, J. R. Cheeseman, J.A. Montgomery Jr, T. Vreven, K. N. Kudin, J. C. Burant, J. M. Millam, S. S. Iyengar, J. Tomasi, V. Barone, B. Mennucci, M. Cossi, G. Scalmani, N. Rega, G.A. Petersson, H. Nakatsuji, M. Hada, M. Ehara, K. Toyota, R. Fukuda, J. Hasegawa, M. Ishida, T. Nakajima, Y. Honda, O. Kitao, H. Nakai, M. Klene, X. Li, J.E. Knox, H.P. Hratchian, J.B. Cross, V. Bakken, C. Adamo, J. Jaramillo, R. Gomperts, R.E. Stratmann, O. Yazyev,

ACCEPTED MANUSCRIPT

A.J. Austin, R. Cammi, C. Pomelli, J.W. Ochterski, P.Y. Ayala, K. Morokuma, G.A. Voth, P. Salvador, J. J. Dannenberg, V.G. Zakr-zewski, S. Dapprich, A.D. Daniels, M.C. Strain, O. Farkas, D. K. Malick, A.D. Rabuck, K. Raghavachari, J.B. Foresman, J.V. Ortiz, Q. Cui, A.G. Baboul, S. Clifford, J. Cioslowski, B. B. Stefanov, G. Liu, A. Liashenko, P. Piskorz, I. Komaromi, R. L. Martin, D. J. Fox, T. Keith, M.A. Al-Laham, C.Y. Peng, A. Nanayakkara, M. Challacombe, P. M.W. Gill, B. Johnson, W. Chen, M.W. Wong, C. Gonzalez, J.A. Pople, Gaussian 03, Revision C02, Gaussian Inc., Pittsburgh, PA, 2004.

[51] X. Yang, L. Zheng, L. Xie, Z. Liu, Y. Li, R. Ning, G. Zhang, X. Gong, B. Gao, C. Liu. 207 (2015) 9-24.

[52] S. Suganya, J. S. Park and S. Velmathi, *Sensors and Actuators B.* 190 (2014) 679-684.

ACCEPTED MANU

ACCEPTED MANUSCRIPT

Highlights

- Colorimetric responses of S1-S4 to anions in organic (DMSO) and organo: aqueous (DMSO:water) medium were visible to the naked eye
- Detection of F- and CN- by S1-S4 was monitored by means of UV-vis and test stripes techniques.
- The S1-S4 ha an excellent sensitivity with the detection limits under micro molar concentration
- The method was validated and applied for the detection F- ion in real samples(mouth freshener and toothpaste).

ACCEPTED MANUSCRIPT